# Phase-sensitive method for background-compensated photoacoustic detection of $NO_2$ using high-power LEDs

**Jaakko Saarela,**[1,*] **Tapio Sorvajärvi,**[1] **Toni Laurila,**[2] **and Juha Toivonen**[1]

[1]*Optics Laboratory, Department of Physics, Tampere University of Technology, P.O. Box 692, FI-33101 Tampere, Finland*

[2]*Centre for Metrology and Accreditation, P.O. Box 9, FI-02151 Espoo, Finland*

[*]*jaakko.saarela@tut.fi*

**Abstract:** A photoacoustic (PA) sensor has been developed for the detection of nitrogen dioxide ($NO_2$). Ten amplitude-modulated high-power light emitting diodes (LEDs), emitting a total optical power of 9 W at 453 nm, are used to excite the photoacoustic signal in $NO_2$. The LEDs are attached to the circumference of a cylindrical PA cell. The induced longitudinal acoustics waves are detected using two electromechanical film stacks, located at the ends of the cell. Background signal cancelation is achieved by using phase-sensitive detection of the difference signal of the two pressure transducers. The phase-sensitive approach allows for improved dynamic range and sensitivity. A detection limit of 10 parts per billion by volume was achieved for flowing $NO_2$ gas sample in an acquisition time of 2.1 s, corresponding to a minimum detectable absorption coefficient of $1.6 \times 10^{-7}$ cm$^{-1}$Hz$^{-1/2}$. The developed sensor has potential for compact, light-weight, and low-cost measurement of $NO_2$.



**OCIS codes:** (300.6430) Spectroscopy, photothermal; (300.6380) Spectroscopy, modulation; (230.3670) Light-emitting diodes; (120.5475) Pressure measurement; (120.5050) Phase measurement.

## References and links

1. A. Rosencwaig, *Photoacoustics and Photoacoustic Spectroscopy* (Robert E. Krieger Publishing Company, 1980).
2. "Our Nation's Air–Status and Trends through 2008," Tech. Rep., U.S. Environmental Protection Agency (2010).
3. J. H. Shorter, S. Herndon, M. S. Zahniser, D. D. Nelson, J. Wormhoudt, K. L. Demerjian, and C. E. Kolb, "Real-time measurements of nitrogen oxide emissions from in-use New York City Transit buses using a chase vehicle," Environ. Sci. Technol. **39**, 7991–8000 (2005).
4. P. C. Claspy, C. Ha, and Y.-H. Pao, "Optoacoustic detection of $NO_2$ using a pulsed dye laser," Appl. Opt. **16**, 2972–2973 (1977).
5. J. Saarela, J. Sand, T. Sorvajrvi, A. Manninen, and J. Toivonen, "Transversely excited multipass photoacoustic cell using electromechanical film as microphone," Sensors **10**, 5294–5307 (2010).
6. A. Manninen, J. Sand, J. Saarela, T. Sorvajärvi, J. Toivonen, and R. Hernberg, "Electromechanical film as a photoacoustic transducer," Opt. Express **17**, 16994–16999 (2009).
7. N. Barreiro, A. Vallespi, A. Peuriot, V. Slezak, and G. Santiago, "Quenching effects on pulsed photoacoustic signals in $NO_2$-air samples," Appl. Phys. B: Lasers Opt. **99**, 591–597 (2010).
8. R. Bartlome, M. Kaučikas, and M. W. Sigrist, "Modulated resonant versus pulsed resonant photoacoustics intrace gas detection," Appl. Phys. B **96**, 561–566 (2009).
9. V. Slezak, "High-precision pulsed photoacoustic spectroscopy in $NO_2$-$N_2$," Appl. Phys. B: Lasers Opt. **73**, 751–755 (2001).

#145946 - $15.00 USD Received 14 Apr 2011; revised 18 May 2011; accepted 19 May 2011; published 26 May 2011

10. V. Slezak, G. Santiago, and A. L. Peuriot, "Photoacoustic detection of $NO_2$ traces with CW and pulsed green lasers," Opt. Lasers Eng. **40**, 33–41 (2003).
11. H. Yi, K. Liu, W. Chen, T. Tan, L. Wang, and X. Gao, "Application of a broadband blue laser diode to trace $NO_2$ detection using off-beam quartz-enhanced photoacoustic spectroscopy," Opt. Lett. **36**, 481–483 (2011).
12. J. Kalkman and H. van Kesteren, "Relaxation effects and high sensitivity photoacoustic detection of $NO_2$ with a blue laser diode," Appl. Phys. B: Lasers Opt. **90**, 197–200 (2008).
13. M. Pushkarsky, A. Tsekoun, I. G. Dunayevskiy, R. Go, and C. K. N. Patel, "Sub-parts-per-billion level detection of $NO_2$ using room-temperature quantum cascade lasers," Proc. Natl. Acad. Sci. U.S.A. **103**, 10846–10849 (2006).
14. J. Lima, H. Vargas, A. Mikls, M. Angelmahr, and P. Hess, "Photoacoustic detection of $NO_2$ and $N_2O$ using quantum cascade lasers," Appl. Phys. B: Lasers Opt. **85**, 279–284 (2006).
15. R. Bernhardt, G. D. Santiago, V. B. Slezak, A. Peuriot, and M. G. Gonzlez, "Differential, LED-excited, resonant $NO_2$ photoacoustic system," Sens. Actuators B **150**, 513–516 (2010).
16. G. D. Santiago, M. G. Gonzalez, A. L. Peuriot, F. Gonzalez, and V. B. Slezak, "Blue light-emitting diode-based, enhanced resonant excitation of longitudinal acoustic modes in a closed pipe with application to $NO_2$," Rev. Sci. Instrum. **77**, 023108 (2006).
17. K. Bogumil, J. Orphal, T. Homann, S. Voigt, P. Spietz, O. C. Fleischmann, A. Vogel, M. Hartmann, H. Kromminga, H. Bovensmann, J. Frerick, and J. P. Burrows, "Measurements of molecular absorption spectra with the SCIAMACHY pre-fight model: instrument characterization and reference data for atmospheric remote-sensing in the 2302380 nm region," J. Photochem. Photobiol., A **157**, 167–184 (2003).
18. V. Sivakumaran, K. P. Subramanian, and V. Kumar, "Self-quenching and zero-pressure lifetime studies of $NO_2$ at 465-490, 423-462 and 399-416 nm," J. Quant. Spectrosc. Radiat. Transf. **69**, 525–534 (2001).
19. R. A. Gangi and L. Burnelle, "Electronic structure and electronic spectrum of nitrogen dioxide. III Spectral interpretation," J. Chem. Phys. **55**, 851–856 (1971).
20. C. M. Roehl, J. J. Orlando, G. S. Tyndall, R. E. Shetter, G. J. Vazquez, C. A. Cantrell, and J. G. Calvert, "Temperature dependence of the quantum yields for the photolysis of $NO_2$ near the dissociation limit," J. Chem. Phys. **98**, 7837–7843 (1994).
21. A. Manninen, "Pulsed Laser Spectroscopy: Bioaerosol Fluorescence and Gas-Phase Photoacoustics," Ph.D. thesis, Tampere University of Technology (2009).
22. M. Paajanen, J. Lekkala, and K. Kirjavainen, "Electromechanical film (EMFi)–a new multipurpose electret material," Sens. Actuators, A **84**, 95–102 (2000).
23. Y.-H. Pao, P. C. Claspy, C. F. j. Dewey, J. A. Gelbwachs, P. L. Kelley, L. B. Kreuzer, M. B. Robin, A. Rosencwaig, J. D. Stettler, and N. M. Witiriol, *Optoacoustic Spectroscopy and Detection* (Academic Press, Inc., 1977).
24. A. Miklós, P. Hess, and Z. Bozóki, "Application of acoustic resonators in photoacoustic trace gas analysis and metrology," Rev. Sci. Instrum. **72**, 1937–1955 (2001).
25. A. Kosterev, Y. Bakhirkin, F. Tittel, S. Blaser, Y. Bonetti, and L. Hvozdara, "Photoacoustic phase shift as a chemically selective spectroscopic parameter," Appl. Phys. B: Lasers Opt. **78**, 673–676 (2004).
26. G. Z. Angeli, Z. Bozoki, A. Miklos, A. Lorincz, A. Thony, and M. W. Sigrist, "Design and characterization of a windowless resonant photoacoustic chamber equipped with resonance locking circuitry," Rev. Sci. Instrum. **62**, 810–813 (1991).

## 1. Introduction

Photoacoustic spectroscopy (PAS) is an established and sensitive method for trace gas monitoring. It is based on the photoacoustic (PA) effect where modulated light is absorbed by gas molecules and converted to sound by non-radiative relaxation of the excited energy levels of the molecules. The induced sound waves are detected with a microphone. [1]

Nitrogen dioxide ($NO_2$) is an atmospheric pollutant which is mainly emitted into the atmosphere from anthropogenetic sources, such as combustion processes. The average mixing ratio of $NO_2$ in the atmosphere is typically between $5-30$ parts per billion by volume (ppb) [2] but can be orders of magnitude higher close to its source [3]. PAS has been previously applied to the detection of $NO_2$ using pulsed dye lasers [4], solid-state lasers [5–10], semiconductor diode lasers [11, 12], quantum cascade lasers [13, 14], and light emitting diodes (LEDs) [15, 16]. Since the PA signal is directly proportional to the excitation power [1], it is favorable to use high-power light sources for excitation. In the visible spectral range modern high-power LEDs offer an attractive alternative by reaching power levels beyond 1 W. Combined with low-cost microphone technology, LED-based PA sensors provide an interesting and cost-effective solution for $NO_2$ monitoring.

#145946 - $15.00 USD Received 14 Apr 2011; revised 18 May 2011; accepted 19 May 2011; published 26 May 2011

$NO_2$ has a strong and broadband absorption spectrum covering the $250-650$ nm spectral range with a maximum absorption cross-section of $7.4\times10^{-19}$ cm$^2$/molecule at 414 nm [17]. The zero-pressure fluorescence lifetime of $NO_2$ in the excitation band of $423-464$ nm is approximately 43 $\mu$s [18], whereas the non-radiative lifetime is less than 4 $\mu$s at atmospheric pressure [12]. Thus, approximately 90 % of the absorbed light energy is expected to be converted to pressure through the PA effect. However, below 415 nm photochemical dissociation of $NO_2$ occurs [19, 20], which has been observed to reduce the PA signal by about 30 % at 510 Hz modulation frequency [1] and even more so at higher frequencies [21]. Therefore, excitation at slightly longer wavelengths is preferable, although high-power LEDs are available around the peak absorption of $NO_2$.

In this work sensitive PA detection of $NO_2$ is demonstrated using an array of ten amplitude-modulated high-power LEDs, emitting a total power of 9 W around 453 nm. The LEDs illuminate a cylindrical PA cell and excite its second longitudinal acoustic mode at 3.9 kHz resonance frequency. The induced pressure waves are detected with two stacks of five-layer electromechanical (EMFIT) films that are attached to the ends of the PA cell. EMFIT film microphones have recently been introduced for PAS of gases as a low-cost, light-weight, and wide-bandwidth alternative for condenser microphones [5, 6]. The EMFIT microphones are flexible, 70-$\mu$m-thick polymer films having ferroelectric properties [22]. Thin metal electrodes on both sides of the film stack allow the extraction of the pressure-induced electric signal. In this study, the two EMFIT stacks are oriented in such a way that the internal electric polarizations are in opposite directions. This novel construction results in a 180° phase difference between the two microphone signals. By monitoring their difference, common-mode electrical or vibrational disturbances are canceled.

PA background signal is a common drawback in systems using amplitude-modulated high-power light sources. The background signal stems from light being absorbed to the walls and windows of the measurement cell. If the background signal is in phase with the induced PA signal from the gas, a simple background subtraction technique can be applied. However, if the PA background has an opposite-phase component, the dynamic range and detection limit of a PA detector can be limited [23]. A common method to reduce such unwanted background signals is to use acoustic filters [24]. In this study, the remaining PA background in the difference signal was observed to originate from the high-power LEDs. This background can be distinguished from the PA signal of $NO_2$ using phase-sensitive detection. Finally, it is demonstrated that the phase of the PA signal can also be used to track the frequency of the acoustic resonance which drifts due to changes in the gas temperature.

## 2. Photoacoustic cell with high-power LEDs

The schematic of the PA sensor is shown in Fig. 1. Two five-layer EMFIT film microphones seal the ends of the cylindrical resonator, made of acrylic plastic. The length and inner diameter of the resonator are 9.0 cm and 3.6 cm, respectively. The quality factor ($Q$) of the PA cell was measured to be 50 at the second longitudinal mode of 3.9 kHz. The microphones were constructed by gluing five circular sheets of EMFIT films together so that their permanent internal polarizations were orientated in the same direction. Stacking five films together yields approximately five-fold sensitivity [5]. Finally, the two film stacks were attached onto grounded aluminum back-plates with positive and negative electrodes facing each other which results in 180° phase difference between their acoustic responses. By measuring the difference of the microphone signals, common-mode electrical or vibrational disturbances are eliminated while the overall signal is doubled.

#145946 - $15.00 USD Received 14 Apr 2011; revised 18 May 2011; accepted 19 May 2011; published 26 May 2011

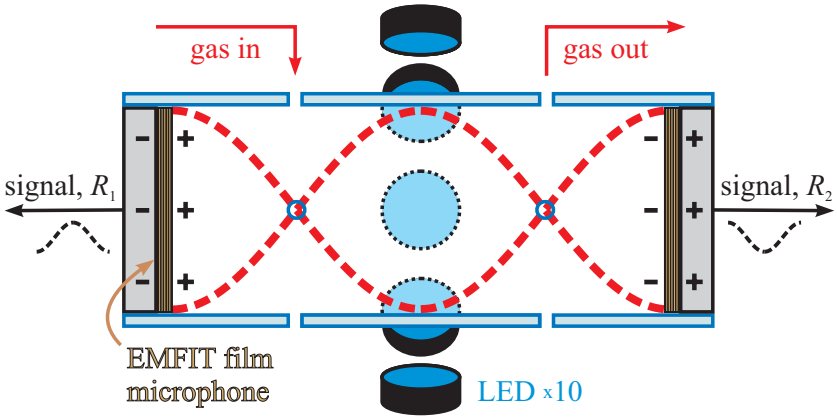


Fig. 1. Photoacoustic (PA) cell. Ten blue (453 nm) high-power LEDs are attached to the central part of the cell to excite acoustic waves at the second longitudinal mode when $NO_2$ is present. $NO_2$ monitoring is accomplished by measuring the difference of the opposite-phase PA signals of two EMFIT film microphones.

Ten blue high-power LEDs (LDW5AM-3T-4-0, OSRAM Opto Semiconductors) with metal-core printed circuit boards are attached onto the decahedron-shaped inner surface of the PA cell's aluminum body. The body functions both as a heat sink for the LEDs and an acoustic enclosure. The distance from the LEDs to the inner surface of the acrylic resonator tube is approximately 3.5 cm. The LEDs are close to Lambertian light sources with highly diverging emission. The full width at half maximum (FWHM) angle of the emission pattern is approximately 120°. The diverging emission was collimated using a plastic (polymethylmethacrylate, PMMA) lens

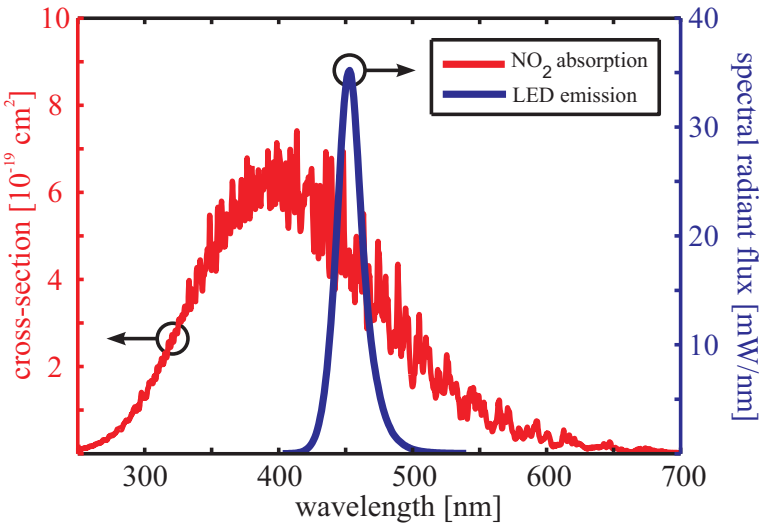


Fig. 2. Absorption cross-section of nitrogen dioxide [17], and the emission spectrum of a high-power LED.

#145946 - $15.00 USD Received 14 Apr 2011; revised 18 May 2011; accepted 19 May 2011; published 26 May 2011

(LO2-RS, Ledil) into a FWHM angle of 7°. The collimation efficiency was measured with an integrating sphere and it was over 90 % for the particular lens used. The peak wavelength, linewidth, and the delivered emission power at 1 A electric peak current were 453 nm, 23 nm, and 900 mW, respectively. The spectral emission of one LED is shown in Fig. 2 together with the absorption cross-section of $NO_2$. The effective absorption cross-section within the LED emission profile is $4.5 \times 10^{-19}$ cm$^2$/molecule, calculated for an optically thin $NO_2$ gas as the average cross-section weighted by the LED emission spectrum.

Square-wave-modulated electric current is provided to the series-connected LEDs through an in-house built current driver that is controlled with a function generator (33250A, Agilent Technologies). The gas sample is diluted from 308 ppm $NO_2$–$N_2$ mixture (AGA) using a cascade of two mass flow controller units (5850S, Brooks Instrument). The gas is fed into the resonator through four 1-mm-sized holes that are located at the nodal points of the second eigenmode, minimizing the coupling of ambient acoustic noise into the PA cell.

## 3. Photoacoustic signal

The generation of the difference PA signal is illustrated in Fig. 3. Both the absorbing $NO_2$ molecules $(R_\mathrm{s})$ and the background $(R_\mathrm{b})$ contribute to the PA signal. In general, the two PA signal components, $R_\mathrm{s}$ and $R_\mathrm{b}$, have a fixed phase difference $\theta$, which describes the delay between the PA signal from $NO_2$ and the background. The delay can arise either from different relaxation rates at which the two sound waves are produced or from the difference in their acoustic propagation path lengths. Here, the non-radiative relaxations are fast compared to the modulation period, and thus, only the propagation delay has an effect on the phase $\theta$.

Neglecting common-mode in-phase components the two microphone signals can be expressed as $R_1 = \left(R_{s1}\mathrm{e}^{\mathrm{i}\theta} + R_{b1}\right)\mathrm{e}^{\mathrm{i}\phi}$, and $R_2 = \left(R_{s2}\mathrm{e}^{\mathrm{i}\theta} + R_{b2}\right)\mathrm{e}^{\mathrm{i}(\pi+\phi)}$, where $\phi$ is a frequency-dependent PA signal phase which is caused by the longitudinal acoustic resonance and is the same for both the PA signal and background. Assuming equal microphone sensitivities, the magnitudes $R_{s1} = R_{s2} = R_\mathrm{s}$ and $R_{b1} = R_{b2} = R_\mathrm{b}$. Hence, the difference PA signal is $R_1 - R_2 = 2\left(R_\mathrm{s}\mathrm{e}^{\mathrm{i}\theta} + R_\mathrm{b}\right)\mathrm{e}^{\mathrm{i}\phi}$. The measurement delay can be adjusted, i.e. the reference coordinate system can be rotated, in such a way that $\phi = 0$ at the resonance of the PA cell. Then, as depicted in Fig. 3 a, the background becomes purely real, and the $NO_2$ signal projection is achieved from the imaginary part of the resultant PA signal. Kosterev et al. have used a similar

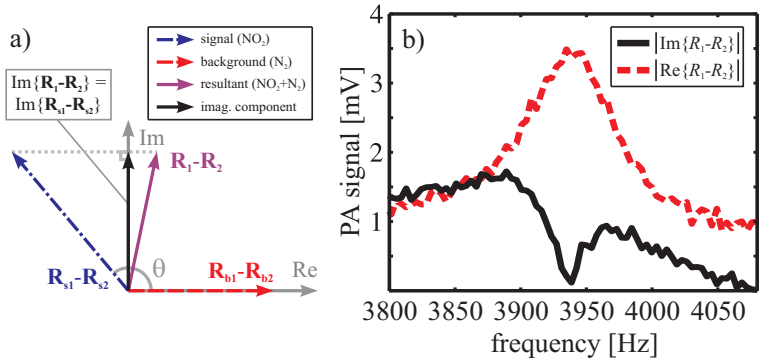


Fig. 3. Generation of the difference PA signal. **(a)** The resultant signal has only components of PA origin. Background-free measurement of $NO_2$ is achieved from the imaginary component. **(b)** Measured PA backgrounds from an empty ($N_2$-filled) cell. At the resonance of the PA cell (3940 Hz) the imaginary component of the PA background signal is reduced to the combined noise level of the two microphones.

#145946 - $15.00 USD Received 14 Apr 2011; revised 18 May 2011; accepted 19 May 2011; published 26 May 2011

phase-sensitive approach to distinguish between two gases, which have overlapping absorption features but different non-radiative lifetimes [25].

The opposite-phase PA signals $R_1$ and $R_2$ are amplified by 60 dB and then digitized with a 2-channel oscilloscope (NI USB-5133, National Instruments) using a sampling rate and data record length of 1 MS/s and $2^{19}$, respectively. The PA signals are processed using a LabVIEW program. Four difference PA signals are averaged, yielding a data acquisition time of 2.1 s, and the fast-Fourier transformation (FFT) is calculated to retrieve the PA signal magnitude and phase. The real and imaginary components of PA signals are commonly separated using a lock-in amplifier. Alternatively, they can be calculated from the complex-valued FFT spectrum as done here.

It was observed that the high-power LEDs generate audible background noise when driven at kHz frequencies. The background noise $(R_b)$ is coupled to the acoustic resonance $(3940\ \mathrm{Hz})$ of the PA cell, even with the cell being filled with pure $N_2$, as shown with the dashed line in Fig. 3 b. However, this background signal can be distinguished from the PA signal of $NO_2$ due to the phase shift of 130°, caused by the different propagation lengths in the cell. At the resonance frequency $\phi = 0$ and the background is real, and therefore, the background is eliminated from the imaginary component of the PA signal which is shown with the solid line in Fig. 3 b. Continuous background-compensated monitoring of $NO_2$ concentration is achieved if the modulation frequency of the LEDs is kept at the resonance of the PA cell.

The PA background could also be compensated by using extra LEDs of different color that are modulated with an opposite phase [15]. However, with the presented method the PA background is automatically eliminated by measuring the imaginary PA signal component instead of the resultant, and no extra components are needed. Yet, the method of using extra LEDs of different color and opposite-phase modulation could be used to eliminate possible interference from other atmospheric compounds which absorb visible light, such as ozone and soot particles.

## 4. Results

The PA signal was measured as a function of $NO_2$ concentration both from the resultant amplitude and from the imaginary component of the complex difference signal. The open data points in Fig. 4 show resultant PA signal in the presence of 3.5 mV PA background. The phase of the PA background lags 130° with respect to the PA signal from $NO_2$ as can be seen from the inset of Fig. 4. This corresponds to an acoustic path length of 3.3 cm which approximately matches the distance from the LEDs to the outer surface of the acrylic resonator tube. This implies that the LEDs themselves were the source of the PA background instead of the light absorption at plastic walls of the resonator tube. Due to the phase lag the PA response dips around 300 ppb, whereafter the PA signal increases monotonically. Because the phase lag is more than 90°, background-subtraction technique does not improve the limit of detection.

The linear regime is extended to the combined electrical noise floor of the two microphones by measuring the imaginary component of the difference PA signal. Only 25 % of the PA signal is lost from the imaginary part due to the phase difference between the signal from $NO_2$ and background. This reduction could be avoided by re-designing the PA cell so that the LEDs would be located at exactly a quarter wavelength, which is 2.25 cm, apart from the acoustic resonator. In-phase PA background, which would arise from light absorption at the plastic cylinder walls and be larger than the measured electrical noise, was not observed. In fact, even if a small-amplitude in-phase PA background component existed, the detection phase could be fine-tuned in such a way that the resultant PA background would again be balanced out from the imaginary part of the PA signal. The noise level (80 $\mu$V) was measured as the root-mean-square (RMS) noise of the imaginary component from pure $N_2$ at the 2$^{nd}$ longitudinal resonance of the PA cell while the LEDs were being modulated. The detection limit for $NO_2$ in $N_2$ matrix is

#145946 - $15.00 USD Received 14 Apr 2011; revised 18 May 2011; accepted 19 May 2011; published 26 May 2011

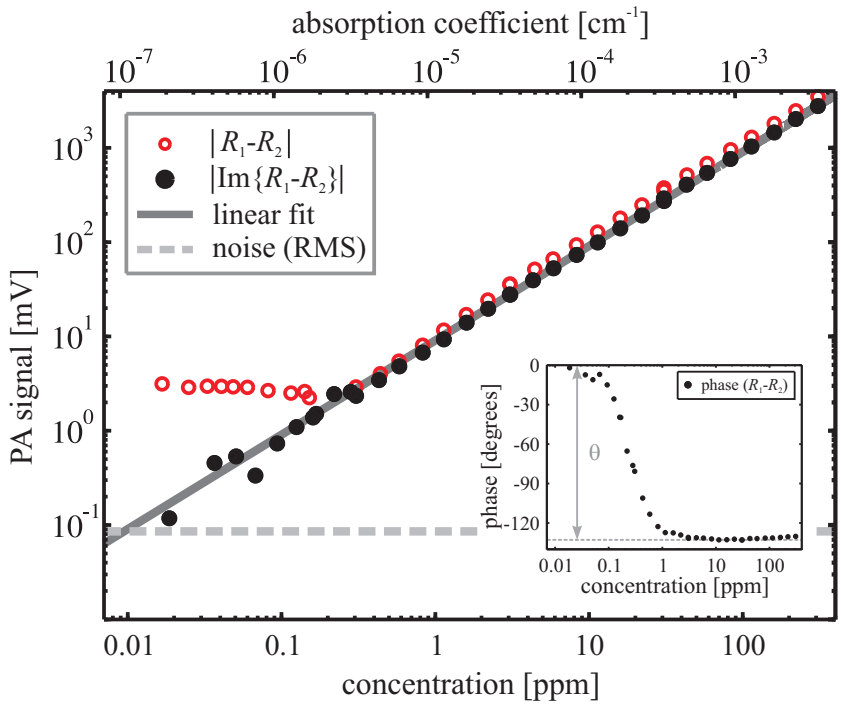


Fig. 4. PA signal as a function of $NO_2$ concentration. Open circles represent the PA signal in the presence of 3.5 mV background. The linear dynamic range is extended to the noise floor by measuring the imaginary component of the PA difference signal. The detection limit with 2.1 s acquisition time is 10 ppb. Inset: Phase of the resultant PA signal. Due to the phase difference $\theta = 130^\circ$ background-free measurement of $NO_2$ is achieved from the imaginary component.

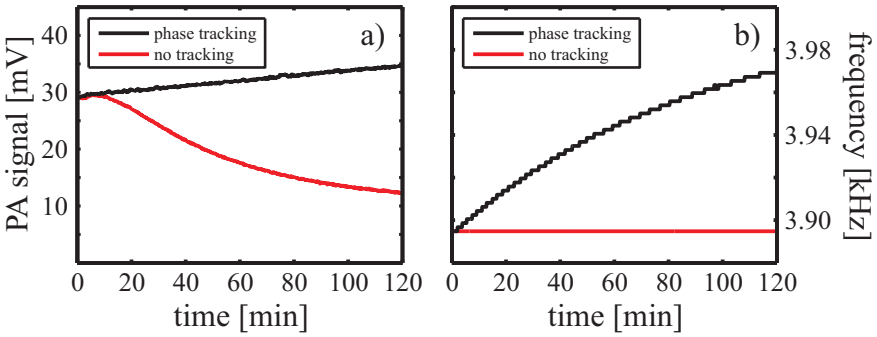


Fig. 5. Imaginary part of the PA signal as a function of time, measured from a constant 3 ppm $NO_2$ concentration **(a)**, and the corresponding signal frequencies **(b)**. The PA cell is heated by the high-power LEDs from 25°C to 40°C, causing the resonance frequency to drift to higher frequencies. Without resonance tracking the PA signal is lost (red curves). The resonance tracking enables continuous monitoring of $NO_2$ (black curves). The increase in PA signal is related to temperature-dependent sensitivity of the microphones.

#145946 - $15.00 USD Received 14 Apr 2011; revised 18 May 2011; accepted 19 May 2011; published 26 May 2011

10 ppb (SNR= 1) with 2.1 s data acquisition time which corresponds to a minimum detectable absorption coefficient of $1.1 \times 10^{-7}$ cm$^{-1}$ or $1.6 \times 10^{-7}$ cm$^{-1}$Hz$^{-1/2}$. The sensitivity of the PA detector is about 180 V/$\left(\text{cm}^{-1}\text{W}\right)$ when normalized with the emitted average power of the LEDs.

During long-term PA measurements temporal changes in the gas temperature can cause problems, especially when using continuous-wave light sources, because the speed of sound is temperature-dependent, and, so is the resonance frequency [24]. In the presented set-up the PA cell itself is heated by the high-power LEDs. Therefore, a feedback algorithm was used to continuously track and minimize the difference between the modulation frequency and the actual resonance of the PA cell. As a demonstration, 3 ppm of $NO_2$ was set to flow at one standard liter per minute through the PA cell, and a signal stability measurement was carried out during which the PA cell temperature increased from 25 to 40°C. The effect of not using any resonance tracking is seen in the decaying PA signal curve of Fig. 5 a which was measured using a fixed modulation frequency of 3,895 Hz. By tracking the resonance frequency of the PA cell from the signal phase, which is $-130^\circ$ at 3 ppm, the PA system followed the drifting resonance. At the same time the PA signal increased slowly by 17 % even though the $NO_2$ concentration was kept constant. The change is related to the increasing sensitivities of the microphone film stacks as a function of temperature, which was experimentally verified using an external loudspeaker. However, this could be easily taken into account by microphone calibration or by controlling the PA cell temperature. It was also checked that the radiant flux of the high-power LEDs reduced only by 1 % as the operating temperature of the PA cell increased. All the PA measurements were carried out in a constant atmospheric pressure, and the $NO_2$ absorption spectrum is not affected by such small temperature changes. It should be noted that the presented method of tracking the resonance directly from the PA signal phase works here only at sample concentrations above 1 ppm where the phase is constant. An additional loudspeaker, driven at some higher harmonic than the 2$^{\text{nd}}$ mode used for PA detection, could be integrated into the PA cell in order to make the resonance tracking concentration-independent [26].

## 5. Conclusion

Photoacoustic detection of $NO_2$ was demonstrated using an array of ten high-power LEDs, which were arranged onto the outer circumference of a transparent cylindrical PA cell. The total emission power and wavelength of the LEDs were 9 W and 453 nm, respectively. The overlapping beams from the LEDs excited pressure waves from $NO_2$ gas at the center of the PA cell. The pressure waves were detected using two stacks of 5-layer electromechanical film microphones. The internal electric polarizations of the film stacks were oriented in opposite directions resulting in opposite-phase PA signals. By measuring the difference of the two microphone signals and by using phase sensitive detection, the background signal that originated from the high-power LEDs, was eliminated improving the linear dynamic range of the PA detector. The minimum detectable absorption coefficient was $1.1 \times 10^{-7}$ cm$^{-1}$ in a measurement time of 2.1 s which corresponds to 10 ppb of $NO_2$ in $N_2$. The developed sensor has potential for compact, light-weight, and low-cost measurement of toxic $NO_2$. The presented PA system could also be modified for the measurement of other atmospheric trace constituents, such as soot particles or ozone, which absorb light in the visible spectral range.

## Acknowledgements

OSRAM Opto Semiconductors GmbH is appreciated for providing the blue high-power LEDs. The authors would like to thank Lic.Sc. Tuomas Poikonen from Aalto University, School of Science and Technology for measuring the spectral radiant flux of the LEDs.

#145946 - $15.00 USD Received 14 Apr 2011; revised 18 May 2011; accepted 19 May 2011; published 26 May 2011